

Linear and Nonlinear Orbit Calculations in Non-isomagnetic Fields

W.-D. Klotz* and R. Maier

Berliner Elektronenspeicherring-Gesellschaft für Synchrotronstrahlung mbH
(BESSY)
Lentzeallee 100. D-1000 Berlin 33

Introduction

The development of compact storage rings which use superconducting air-coil magnets for the bending dipoles has made it necessary to refine the method of existing linear lattice codes. To our knowledge, there exists no linear lattice code that exactly takes into account the strongly non-isomagnetic field shape that is produced by this type of magnet. A set of programs has been developed at BESSY which tackle this problem. These codes are especially useful for studying the influence of insertion devices on the linear particle dynamics.

Reference orbit

In a system with isomagnetic elements, the reference orbit is a simple sequence of straights and arcs. In non-isomagnetic fields the reference orbit has to be calculated by numeric integration. In any magnetic field with midplane symmetry the magnetic field vector is perpendicular to this plane for any point in this plane. Therefore, a charged particle with initial velocity vector parallel to this plane will never leave the plane. The exact motion of the particle is given by the differential equation¹

$$\frac{y'''}{(1+y'^2)^{3/2}} = \frac{e}{P_0} B_z(x,y); y = y(x) \quad (1)$$

with: x, y : cartesian coordinates in the plane
z : cartesian coordinate perpendicular to the plane
y' = dy/dx, y'' = d²y/dx²
e : particle charge
P₀ : particle momentum
B_z : magnetic induction

Transforming equation (1) to polar coordinates, we arrive at the differential equation

$$\frac{r^2 + r'^2 - r r''}{(r^2 - r'^2)^{3/2}} = \frac{e}{p} B_z(r,\phi); r = r(\phi) \quad (2)$$

This equation can easily be transformed to a system of first order differential equations and then be integrated in a given field B_z with given boundary conditions r'(1), r'(2) at the entrance and exit to the magnetic field.

We have studied two different bending magnets with this method. A magnet with a bending angle of 180°, consisting of three banana shaped coils and a similar magnet of 90° bending angle. The magnetic midplane is defined by the symmetrical arrangement of each pair of coils above and below this plane. The magnetic induction B_z in the plane was calculated by a field code for handling general current carrying conductors in three dimensions² by evaluating the Biot-Savart-Law. Fig. 1 shows the top view upon one half of the coil arrangement of the 180° magnet. In the same figure the isomagnetic and non-isomagnetic orbits are shown, too. Due to the symmetry of the magnet, the boundary conditions for the reference orbit have to be set to r'(φ = 0) = r'(φ = 90°) = 0. This orbit represents the ideal equilibrium orbit for a reference particle with momentum P₀.

Field expansion

For calculating the linear particle dynamics we use the expanded form of a magnetic field with midplane symmetry, as has been provided by Brown and Servranckx³. They express the magnetic induction in a general right-handed curvilinear coordinate system (x,y,s) moving with the reference particle.

x : radial coordinate
y : vertical coordinate
s : longitudinal coordinate (and length of reference orbit)

Up to second order this expansion looks like:

$$B_x = A_{11} y + A_{12} x y + \dots = \frac{P_0}{e} [k^2 y + m x y + \dots]$$

$$B_y = A_{10} + A_{11} x + \frac{1}{2!} A_{12} x^2 + \frac{1}{2!} A_{30} y^2 + \dots$$

$$= \frac{P_0}{e} [n + k^2 x + \frac{1}{2!} m x^2 + \frac{1}{2!} (h'' - m - h k^2) y^2 + \dots]$$

$$B_s = \frac{1}{1 + h x} [A_{10}' y + A_{11}' x y + \dots]$$

$$= \frac{P_0}{e} [h' y + (2 k k' - h h') x y + \dots]$$

(a prime means differentiation with respect to s)

with the following multipolefunctions (functions of s!):

$$h(s) = \frac{e}{P_0} B_y \Big|_{x=y=0} = \frac{e}{P_0} A_{10} \quad : \text{dipole};$$

$$k^2(s) = \frac{e}{P_0} \frac{\partial B_y}{\partial x} \Big|_{x=y=0} = \frac{e}{P_0} A_{11} \quad : \text{quadrupole};$$

$$m(s) = \frac{e}{P_0} \frac{\partial^2 B_y}{\partial x^2} \Big|_{x=y=0} = \frac{e}{P_0} A_{12} \quad : \text{sextupole};$$

$$o(s) = \frac{e}{P_0} \frac{\partial^3 B_y}{\partial x^3} \Big|_{x=y=0} = \frac{e}{P_0} A_{13} \quad : \text{octupole};$$

$$d(s) = \frac{e}{P_0} \frac{\partial^3 B_y}{\partial x^3} \Big|_{x=y=0} = \frac{e}{P_0} A_{14} \quad : \text{decapole}.$$

We calculated these multipolefunctions by numerical differentiation of the field along the normal direction of the curved reference orbit. Fig. 2 - 6 show these functions for the 180° bending magnet. The abscissa starts at s = 0 which represents the symmetry point in the middle of the magnet. For the dipole and quadrupole functions the corresponding hard edge model has been indicated as well. As expected, the true field, which is produced by the superconducting air-coil arrangement, deviates drastically from a hard edge model, especially in the entrance and exit regions of the magnet.

* now at ESRF, Grenoble

Linear optics

For the linear particle dynamics only the dipole and quadrupole field functions are needed. A linear optics program called PECOS has been developed. This program calculates twiss functions, chromaticities and radiation integrals $I_1 - I_5$ in the presence of standard isomagnets and non-isomagnets characterized by $h(s)$ and $k^2(s)$. In the program the functions $h(s)$ and $k^2(s)$ are evaluated at arbitrary arguments by third order spline approximations. The characteristic first order trajectories (matrix elements) of the system $[C_i, C_i', S_i, S_i', d_i, d_i' (i = x, y)]$ are integrated by a fourth order Runge-Kutta algorithm. All integrations for averages and radiation integrals around the closed orbit of a circular lattice are evaluated by a 10-point Simpson integration between adjacent points of spline intervals. The differentiation has been performed by a seven point differentiation formula with a minimal step size of 2 mm. For comparison we calculated the optics of two different lattices. The first lattice (A) uses a race-track-shape orbit with two 180° bending magnets and two quadrupoles in each straight section. The second lattice (B) uses four cells with four quadrupoles and one 90° magnet in each cell. We compared the results with calculations where we replaced the non-isomagnetic dipoles by hard edge dipoles. The results of these calculations have been summarized in Fig. 7 and 8, where the β -functions and the horizontal dispersions have been presented and in Table 1, where the corresponding lattice parameters are shown.

Non linear calculation

To take into account the higher order multipole functions, we used the kick approximation. In this approximation the abscissa is divided into intervals and the function in that interval is replaced by a correspondingly adjusted kick of infinitesimal length. Between each kick we used the linear transformation matrices calculated by the method described in the section above. This method, however, does not take into account the dynamic nonlinear parts in the field expansion. The tracking results can be treated by different post-processors which present phase space plots, trajectory plots and Fourier spectra of the betatron motions. As a demonstration of the nonlinear calculations, we show in Fig. 9 the maximal stable emittance for the lattice A. In this case the vertical tune has been fixed and the horizontal tune was scanned. In the presence of only sextupoles the resonances $3Q_x = 4$ and $2Q_y + Q_x = 4$ show up as strong dips. By adding higher multipoles the resonances are shifted and smeared out.

References

- ¹ K.G. Steffen, "High Energy Beam Optics", Interscience Publishers 1965
- ² W.-D. Klotz, R. Maier, "3-D Magnetfeld Berechnung des COSY-Magneten", BESSY TB 71/85 COSY (Januar 1985)
- ³ K.L. Brown, R.V. Servranckx, "First- and Second-order Charged Particle Optics", SLAC-PUB-3381 (July 1984)
- ⁴ W.G. Bickley, "Formulae for Numerical Differentiation", Math. Gaz. 25, 19-27 (1941)

	Lattice A Circumference: 9,6 m; # of cells = 2		Lattice B Circumference: 26,88 m; # of cells = 4	
	isomagn.	non-isom.	isomagn.	non-isom.
<u>Averages over a cell</u>				
<Beta-x>	4.48552	4.45979	3.01398	3.17849
<Gamma-x>	4.19733	4.10436	1.03884	1.08527
<Disp.-x>	1.07664	1.07575	1.04961	1.08146
<Beta-y>	3.42053	3.42220	4.30551	4.94499
<Gamma-y>	3.40911	3.31218	.704651	1.10456
<D _x ² /Beta-x>	.594826	.562012	.383020	.386725
<Beta-x(D _x ' + Alpha*D _x /Beta-x) ² >	2.19785	2.02235	.105922	9.893641E-02
Beta-x MAX	13.1309	13.0249	6.03133	6.45286
Beta-x MIN	.105977	.100726	1.13822	1.11946
Beta-y MAX	10.3715	10.1243	5.95513	7.43513
Beta-y MIN	.125144	.121981	1.71054	.814559
Disp-x MAX	3.18625	3.10371	1.87409	1.93081
Disp-x MIN	-.479585	-.433279	.190445	.196456
Particle energy [MeV]	592.250	592.250	1435.20	1435.20
Particle rigidity [T*m]	1.97725	1.97725	4.78905	4.78905
Gamma	1160.00	1160.00	2809.61	2809.61
Revol. time [s]	3.202202E-08	3.202217E-03	8.966209E-08	8.966208E-08
Momentum compaction	-6.705356E-03	1.418914E-02	6.796584E-02	6.737219E-02
Chromaticity-x nat.	-3.20651	-3.13560	-2.22212	-2.32144
Chromaticity-y nat.	-2.60435	-2.53032	-1.50728	-2.36272
Tune QX	1.19787	1.20001	2.25002	2.22596
Tune QY	1.29144	1.28600	1.25002	1.62044
Radiation Integral I1	-6.437111E-02	.136216	1.82692	1.81097
Radiation Integral I2	14.2800	14.8455	5.24975	5.76368
Radiation Integral I3	32.4546	33.6527	4.38630	5.06559
Radiation Integral I4	1.662347E-02	8.290382E-02	1.27539	1.25439
Radiation Integral I5	62.3055	61.2031	.969322	1.26575
Damping time-x [s]	1.535233E-02	1.483319E-03	1.084096E-03	9.554899E-04
Damping time-y [s]	1.533445E-03	1.475035E-03	8.207221E-04	7.475399E-04
Damping time-z [s]	7.662767E-04	7.354640E-04	3.659130E-04	3.370885E-04
Damping partition (D-Sands)	1.164109E-03	5.584426E-03	.242943	.217637
Energy loss per turn [MeV]	2.473520E-02	2.571482E-02	.313585	.344284
Energy spread	7.660496E-04	7.642154E-04	1.062631E-02	1.096053E-03
Emittance-x [π·m·rad]	2.257109E-05	2.142191E-06	7.393064E-07	8.508708E-07

Table 1: Lattice Parameters

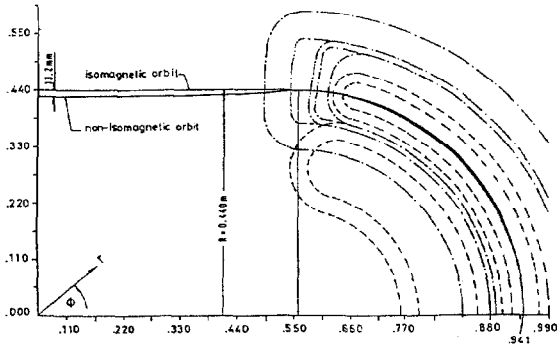


Fig. 1: Top view on the coils arrangement with the isomagnetic and non-isomagnetic orbit.

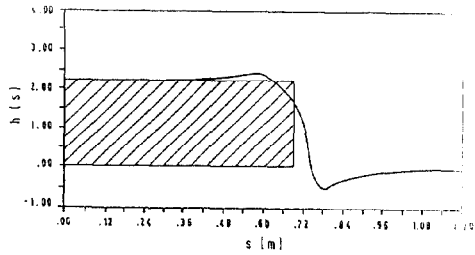


Fig. 2: Dipole function $h(s)$

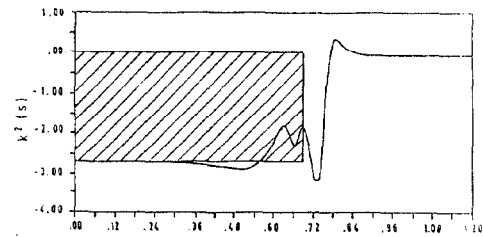


Fig. 3: Gradient function $k^2(s)$

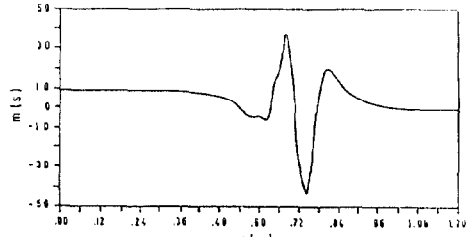


Fig. 4: Sextupole function $m(s)$

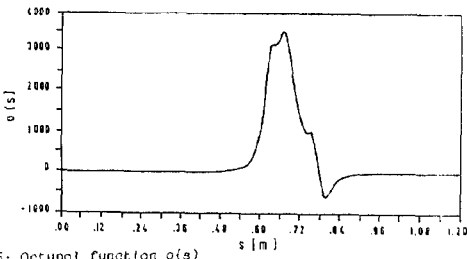


Fig. 5: Octupole function $o(s)$

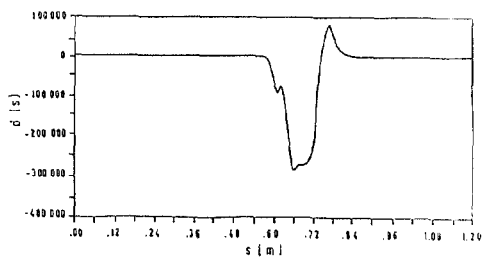


Fig. 6: Decapole function $d(s)$

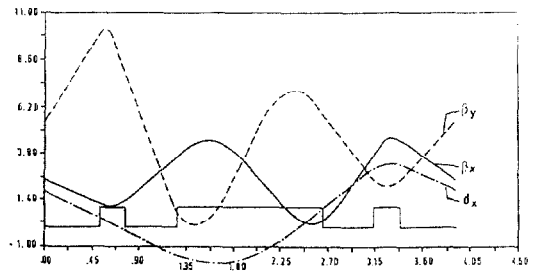


Fig. 7: Twiss functions of Lattice A

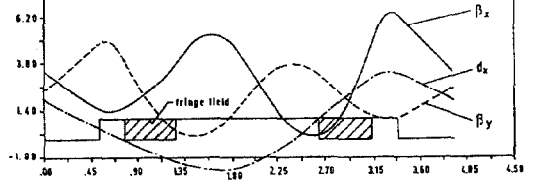


Fig. 7: Twiss functions of Lattice A

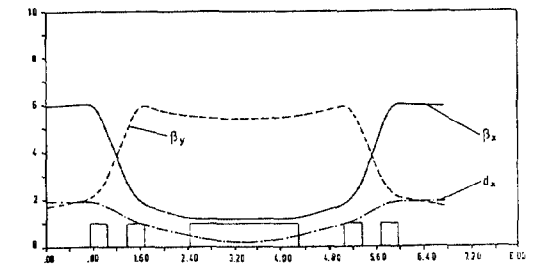


Fig. 8: Twiss functions of Lattice B

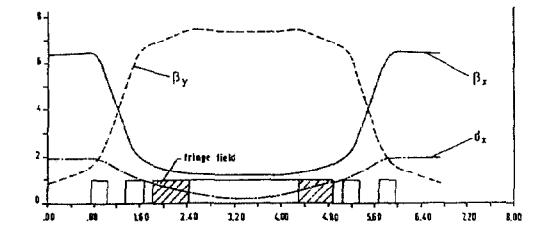


Fig. 8: Twiss functions of Lattice B

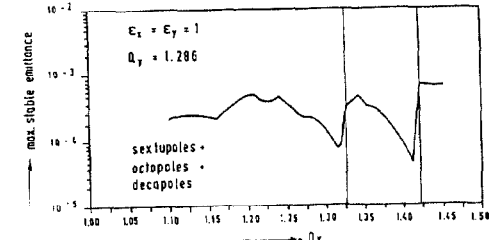
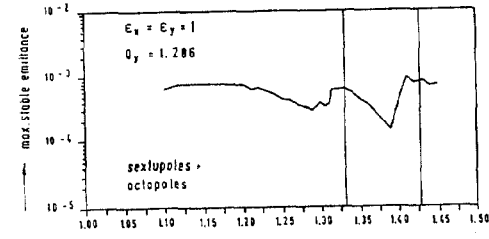
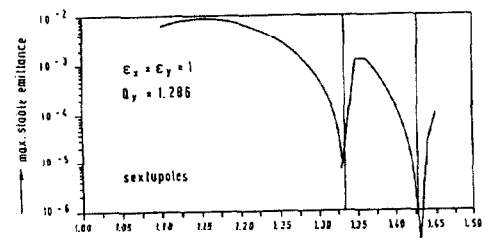


Fig. 9: Horizontal tune vs. maximal stable emittance of Lattice A